Enzyme and Microbial Technology 49 (2011) 153–159

Contents lists available at ScienceDirect

Enzyme and Microbial Technology

journal homepage: www.elsevier.com/locate/emt

Probing fundamental film parameters of immobilized enzymes—Towards enhanced biosensor performance. Part II—Electroanalytical estimation of immobilized enzyme performance

R. Fogel, J.L. Limson*

Department of Biochemistry, Microbiology and Biotechnology, Rhodes University, P.O. Box 94, Grahamstown, South Africa

ARTICLE INFO

Article history:
Received 14 July 2010
Received in revised form 17 February 2011
Accepted 7 May 2011

Keywords:
Enzyme
Immobilization
Kinetics
QCM-D
Biosensor
Viscosity

ABSTRACT

The method of immobilization of a protein has a great influence on the overall conformation, and hence, functioning of the protein. Thus, a greater understanding of the events undergone by the protein during immobilization is key to manipulating the immobilization method to produce a strategy that influences the advantages of immobilization while minimizing their disadvantages in biosensor design.

In this, the second paper of a two-part series, we have assessed the kinetic parameters of thin-film laccase monolayers, covalently attached to SAMs differing in spacer-arm length and lateral density of spacer arms. This was achieved using chronoamperometry and an electroactive product (*p*-benzoquinone), which was modeled in a non-linear regressional fashion to extract the relevant parameters. Finally, comparisons between the kinetic parameters presented in this paper and the rheological parameters of laccase monolayers immobilized in the same manner (Part I of this two paper series) were performed.

Improvements in the maximal enzyme-catalysed current, i_{max}, the apparent Michaelis–Menten constant, K_m and the apparent biosensor sensitivity were noted for most of the surfaces with increasing linker length. Decreasing the lateral density of the spacer-arms brought about a general improvement in these parameters, which is attributed to the decrease in multiple points of immobilization undergone by functional proteins. Finally, comparisons between rheological data and kinetics data showed that the degree of viscosity exhibited by protein films has a negative influence on attached protein layers, while enhanced protein hydration levels (assessed piezoelectrically from data obtained in Paper 1) has a positive effect on those surfaces comprising rigidly bound protein layers.

1. Introduction

The method of protein immobilization has a great impact on conformation, and hence, the kinetic operation of the enzyme, relative to the soluble, 'free', enzyme [1]. These effects can be broadly categorized as: (1) changes occurring due to the non-primary interaction between support and enzyme (hydrostatic, ionic and hydrophobic interactions that occur due to the close proximity of the support to the enzyme) [1–3], (2) changes due to primary interactions occurring between support and enzyme e.g. covalent bond formation and orientation and cross-linked reticulation [2], (3) microenvironmental factors [1,4] and (4) increased diffusional constraints arising from the accumulation of enzyme at selected regions (affecting the rate of substrate interaction with the enzyme and the rate of product release to the transducer/bulk solvent) [1,5]. Additionally, immobilization increases the concentration of biocatalytic protein at the area of attachment, resulting in an increase of protein–protein interactions, altering both microenvironmental and non-primary interactions occurring at the point of immobilization. Alterations in the activity, kinetic stability and Michaelis–Menten constant (compared to free enzyme) have been frequently reported upon immobilization of the enzyme to the solid support, the extent of change being uniquely dependent on the selection of support [5,6], the enzyme in question and method of immobilization [2,3,6–8] used to conjoin the first two elements [1]. Considerable research has been expended into the minimization of deleterious properties while enhancing those properties, such as improved thermostability [4] or pH stability, deemed desirable during immobilization [2,9]. This is often achieved by modulating certain aspects of selected immobilization procedures [2], but many of these papers report only on effects evidenced by the functioning of the protein (i.e. alterations in enzyme kinetics), as opposed to any physical changes undergone by them.

Abbreviations: QCM-D, crystal microbalance with dissipation; SAM, self-assembled monolayer; SLB, succinic-lactic acid buffer, pH 4.5; Glut, glutaraldehyde; Lys, lysin; β-ME, β-mercaptoethanol; Cys, cysteamine; CV, coefficient of variation (C.V.).

* Corresponding author. Tel.: +27 46 603 8441; fax: +27 46 622 3984.
E-mail address: j.limson@ru.ac.za (J.L. Limson).

0141-0229/$ – see front matter © 2011 Elsevier Inc. All rights reserved.
doi:10.1016/j.enzmictec.2011.05.004

Direct observation of conformational changes undergone by immobilized proteins is difficult to achieve, primarily due to the low concentrations of proteins found at the immobilization site and analytical interferences due to the support [1]. Atomic force microscopy has been previously used to analyse both monodispersed and aggregates of proteins attached to supports and used to document attached particles' size and shape (for example in Ref. [10]), but this method (while very useful in assessing surface coverage of a given surface) gives insufficient indication of the extent of denaturation undergone by the protein layer. Quartz-crystal microbalance with dissipation (QCM-D) provides information as to the bound mass, film thickness, viscoelasticity of thin films occurring at electrode surfaces [11], providing an alternative method of probing conformational changes occurring to biomolecules during and after the immobilization process [12], as well as assessing surface coverages and immobilization states of molecules of interest within the biosensor-fabrication paradigm [13].

This paper thus aims to compare both data obtained from measurement of physical parameters of monomolecular layers of protein via the QCM-D (as in Part I of this two paper series) and the kinetic parameters obtained by electroanalysis of products resulting from the activity of laccase within this film.

2. Methods and materials

2.1. Apparatus

Electrochemical measurements were conducted using an Autolab PGSTAT 30 (Eco Chemie), coupled to a VA 336 stand (Metrohm) for stirring control. The working electrodes used in this study were gold-surfaced (Au) electrodes, 0.8 mm geometric radius, sourced from Bioanalytical Systems (BAS). The reference electrode used throughout was an $Ag/AgCl_{sat}$ electrode (BAS). The cell was completed through the use of a platinum wire.

2.2. Reagents

All reagents used were of analytical grade. No further purifications of reagents were undertaken. All water was of milliQ quality (double-distilled). Cysteamine, hydroquinone (HQ), glutaraldehyde (25%, w/v) and 2-mercaptoethanol were sourced from Sigma–Aldrich. Laccase, purified from *Trametes versicolor*, (21.7 U mg^{-1} for catechol at pH 4.5) was sourced from Sigma–Aldrich. All reagents were prepared fresh on a daily basis and stored under dark conditions until used.

2.3. Electrode cleaning

Gold electrodes were polished with alumina oxide for 4 min before being ultrasonicated in absolute ethanol for 2 min. Electrodes were then rinsed with water, before 40 μl of fresh pirhana solution (comprised of 30%, v/v H_2O_2 solution and 95%, v/v H_2SO_4 in a 1:3 proportion) solution were dropped onto the active electrode surface and the electrode surface was chemically etched for a period of 2 min. Electrodes were then rinsed with water and stored in absolute ethanol prior to electrochemical cleaning [14].

Electrochemical cleaning took place by cycling the etched electrodes between −0.25 V and +1.6 V at a rate of 0.2 V s^{-1} in 0.1 M H_2SO_4 until a stable voltammogram was achieved (approx. 100 cycles). Electrodes were then scanned at a scan rate of 0.1 V s^{-1} for approximately 10 scans, or until a stable scan was achieved and the final scan saved for surface area determination (see Section 2.7.1). Electrodes were then reduced in de-aerated ethanol for a period of 30 min, and stored in same until used [14].

2.4. Self assembled monolayer (SAM) formation

Electrodes were modified as in Part I of this two paper series (Table 1) to examine the effect of the differing surface-dependent methods of laccase immobilization on the kinetic parameters of the final laccase films. Stock solutions (100 mM) of β-mercaptoethanol (B-ME) and cysteamine (cys) were made up in milliQ water, de-aerated under N_2 flow and stored at 4 °C and re-made once every 2 days. At any modification, 10 ml of 80%, v/v water: 20%, v/v ethanol (both de-aerated for 10 min) were prepared and degassed for a further 2 min. The two ratios of thiols were then added under N_2 flow. For the 1:4 cys (SAMs 2.1–2.3): B-ME deposition solution, [cys] = 0.4 mM and [B-ME] = 1.6 mM. Similarly, for the 1:99 cys: B-ME (SAMs 1, SAMs 1.1–1.3), [cys] = 0.02 mM and [B-ME] = 1.98 mM.

Electrodes were then introduced to the solution and allowed to modify for at least 8 h in the dark at 4 °C, under sealed conditions. After SAM formation, electrodes were rinsed with successive rinses of ethanol and water and immediately used (i.e. at least 3 rinses per electrode).

Table 1
Compositions of the various surfaces investigated.

SAM number	Cysteamine content (%)	Cysteamine modification[a]
1	1	None
1.1	1	Glut
1.2	1	Glut–lys–glut
1.3	1	Glut–lys–glut–lys–glut
2.1	25	Glut
2.2	25	Glut–lys–glut
2.3	25	Glut–lys–glut–lys–glut
Au	25	None

[a] Layer-by-layer, starting at the basal SAM. "glut" designates glutaraldehyde and "lys" indicates the addition of a lysine residue.

2.5. Modification of the SAM layers

Solutions for the further modification of the SAM layers were prepared in Eppendorf tubes to a final volume of 1 ml. Modifications were performed at room temperature. For glutaraldehyde modification, electrodes were dipped in 1 ml of 1 mM glutaraldehyde solution for a period of 10 min. Thereafter, they were rinsed thoroughly with ethanol and glutaraldehyde-activated SAM modified electrodes were dipped in 1 mM L-lysine. These layers were then activated with glutaraldehyde prior to further modification. Following fabrication of the surfaces, all surfaces were subsequently modified with laccase, as in Section 2.6. The same designations for fabricated biosensors were used as in Part I of this two-paper series (Table 1) and are schematically depicted in Fig. 1.

Briefly: Sensors produced with a basal SAM deposition solution comprised of 1:99 cys: B-ME were designated in this paper as "SAM 1", while those prepared by introduction to a solution of 1:4 cysteamine: β-mercaptoethanol were designated "SAM 2".

A suffix of ".1" indicates activation of the cysteamine residues with glutaraldehyde prior to attachment of laccase. Surfaces labeled as ".2" label the formation of a glutaraldehyde–lysine–glutaraldehyde layer before attachment of laccase. Similarly ".3" labels biosensors fabricated with a double lysine linker connecting the protein to the basal SAM on the electrode (thus, glut–lys–glut–lys–glut linker layer).

2.6. Laccase modification

20 μl of a 4 mg ml^{-1} solution of laccase was dropped onto the active surface of the electrode and allowed to modify for 10 min before being rinsed with water and stored in SLB, pH 4.5 until used (typically within 30 min of modification).

2.7. Electrochemical analyses

2.7.1. Surface area determinations

Real electrode surface area was determined through integration of the gold oxide reduction peak of the final cleaning voltammograms of each electrode in order to determine the charge of that peak. Peak charge was then used to determine the real surface area of the electrode using a value of 400 μC cm^{-2} [14]. From this value, i_{max} and biosensor sensitivity were calculated as an expression of current density (A cm^{-2}), and values of these are displayed and referred to as a function of surface area.

2.7.2. Chronoamperometry

Chronoamperometry was performed under stirred conditions (stirrer speed: 15 000 rpm) using 5 ml of 0.1 M SLB, pH 4.5. The working electrode was poised at −0.05 V (vs. Ag/AgCl) and the current-sampling time was 0.2 s per reading. Aliquots of 50 mM or 100 mM hydroquinone stock solution were used in order to alter the interior concentration of phenolic substrate, and the steady-state current change was recorded and then related to the concentration of phenol.

2.8. Modeling of enzyme kinetics

2.8.1. Electroanalytical modeling system

Immobilized enzyme parameters were determined through non-linear regressional computer modeling. The current response was plotted alongside the substrate concentration, and the theoretical current response was modeled using the following adaptation of the well-known Briggs–Haldane equation [15]

$$I = \left(\frac{I_{max} \times [S]}{K_m + [S]} \right) \quad (1)$$

where I is the total current response at the given substrate concentration (analogous to the enzyme response V, as shown below), I_{max} is the maximal current response (indicative of V_{max}), $[S]$ is the substrate concentration and K_m is the Michaelis–Menten constant of the immobilized enzyme, equivalent to $(k_{-1} + k_{cat})/k_1$.

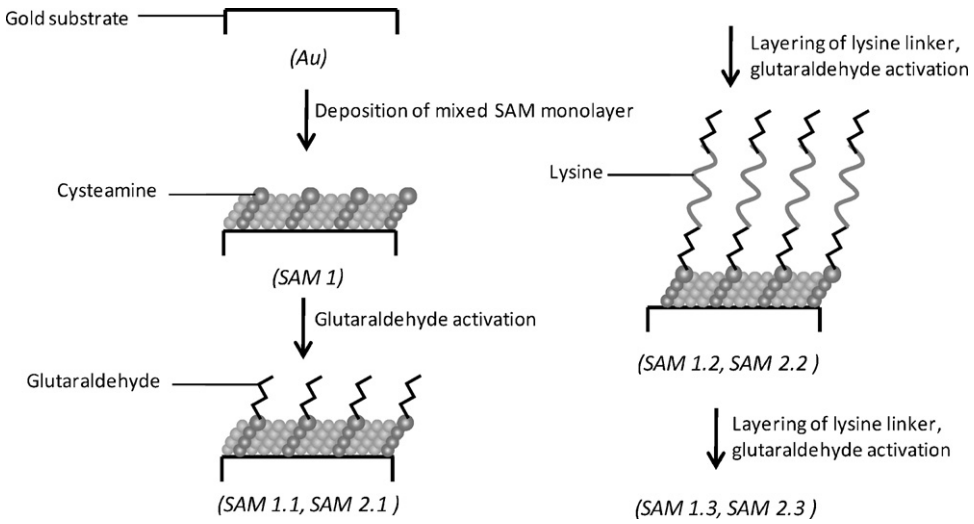

Fig. 1. Schematic diagram representing surfaces used in the course of research presented in this paper. The italicized portions denote the surfaces to which laccase films were attached and subsequently investigated for catalytic performance. SAMs 1 and SAMs 2 differ according to their relative cysteamine: β-mercaptoethanol surface content, as outlined in-text.

For reasons outlined in Section 3, the second scheme was neglected. I_{max} is henceforth reported normalized to electrode surface area, i_{max}, for reasons outlined in Section 3.

Elucidation of the results was performed using Excel Solver Add-in, where iterative values of i_{max} and K_m were altered in order to provide the best "fit" when comparing the theoretical and experimental results. i_{max} and K_m were considered to be accurately estimated when the sum of the square of the differences between theoretical and experimental results reached a minimum, as assessed via the Chi-squared statistic.

The linear response (detection sensitivity) of the biosensor was calculated as the accumulated current density of the sensor between the concentrations of 0 and 40 μM of hydroquinone exposure to the sensor, divided by the concentration of substrate [16].

3. Results and discussion

The selection of laccase as a model biorecognition layer was primarily due to the electrochemically active properties of the products of enzyme reaction. The generation of p-quinone from the enzyme-catalysed oxidation of hydroquinone allows for electrochemical monitoring of product formation, in a similar manner previously outlined in literature [7]. This in turn, provided a highly sensitive reporting system, allowing for sensitive characterisation of the enzyme kinetics even at low surface coverages of functional enzyme molecules, which were anticipated. A satisfactory biorecognition signal was transduced from the surfaces investigated within the nanoampere range (Fig. 2), allowing for accurate modeling of the parameters of the immobilized biomolecule layer to take place (Table 2). An additional criterion for the selection of laccase is that laccases are currently the focus of a great deal of attention for the kinetics of thin-layer enzyme–surface systems (for e.g. inclusion as catalysts for fuel cell cathodes for implantable bioelectrochemical system [19,20] and for biosensing applications [21,22].

Table 2
Operational kinetics parameters determined for immobilized laccase films with regard to the detection of HQ.

Surface	Detection sensitivity (nA μM^{-1} cm^{-2})	i_{max} (nA cm^{-2})	K_m (μM)
Au	3.94 ± 0.53	429 ± 86	132 ± 19
SAM 1	2.59 ± 0.29	544 ± 44	224 ± 29
SAM 1.1	4.77 ± 0.86	1009 ± 57	205 ± 24
SAM 1.2	8.42 ± 0.49	808 ± 85	95 ± 18
SAM 1.3	11.8 ± 0.75	1404 ± 105	101 ± 3
SAM 2.1	2.32 ± 0.17	404 ± 28	196 ± 8
SAM 2.2	4.52 ± 0.40	495 ± 57	127 ± 21
SAM 2.3	5.30 ± 0.29	677 ± 41	112 ± 14

Uncertainties represent standard deviations from the mean. Number of independent measurements, $n \geq 3$.

3.1. Data gathering, treatment and modeling

The SDS wash stage following protein immobilization (Part I of this series) was used exclusively for QCM-D analysis in order to remove loosely bound proteins from the film. It should be stressed that this was not considered necessary for the fabrication of the electrochemical biosensor, due to the rapid washing of the modified electrode using large volumes of water and buffer, neither of which are readily utilizable using QCM-D without causing signal perturbation.

Since the transduced current of the biosensor is in the sub- to low-μA range, the substrate turnover is estimated to be in the pmol min^{-1} range) when using substrate concentrations starting at the μM range. Hence, steady-state enzyme kinetics were assumed to dominate and enzyme kinetics modeling proceeded as normal, as the total change in substrate concentration throughout the analysis was assumed to be far less than 1% of the bulk substrate

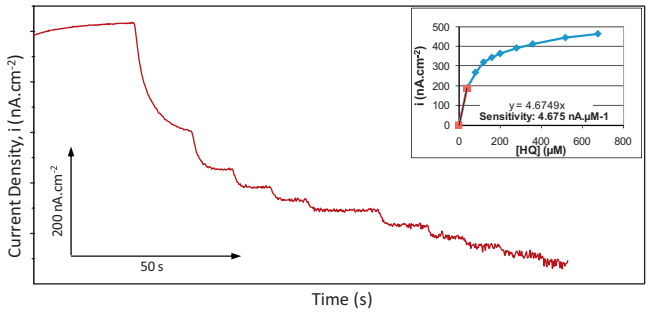

Fig. 2. Chronoamperogram (current values adjusted to account for surface area) generated through the use of laccase immobilized to a gold electrode through the use of SAM 1.1. Scales of the current-time values for this biosensor are represented in the bottom-left corner. Grey single-headed arrows indicate the time of the addition of 2.5 μl of 80 mM HQ (an increase in concentration of approximately 50 μM) and the double-headed arrows indicate the addition of 5 μl of the same concentration of HQ. Inset diagram: The current-concentration curve drawn from these data, and the K_m, biosensor sensitivity and i_{max} (V_{max}) values determined from same from use of the modeling software.

concentration (in fact, a factor of at least 10^4 separated the bulk solution from the velocity of enzyme reaction). This, coupled with the fact that the reduction of p-benzoquinone regenerated hydroquinone at the electrode surface, indicated that no significant alteration in the composition of the bulk substrate occurred over the time-period in which analysis occurred.

Although laccase makes use of dioxygen as the final electron acceptor (transferring electrons gained from the oxidation of phenolic substrates to produce water), it was not considered to be necessary for inclusion within the modeling process. Two interrelated reasons are proffered for this: firstly, that the stoichiometry of reaction is 4 phenolic substrates for a single oxygen turnover and hence that for the reduction of dioxygen to water to be significantly affected, the entire reaction undergone should be greater than 4 times that of the rate of the equilibrium-kinetics of the first phase of the enzymatic reaction. Secondly, and more importantly, the low current response of the biosensor indicated that the depletion of oxygen at the enzyme-layer was not significant enough to warrant inclusion within the model.

Fig. 1 shows a typical chronoamperogram (and associated current-concentration profile) produced by the reduction of laccase-catalysed 1,4-benzoquinone reduction at the electrode surface.

As Fig. 1 demonstrates, a rapid current response (>10 s) to changes in substrate concentration is noted (from stable current-baseline to stable baseline) when using this electrode. However, it provides a very low sensor response, and suffers from a particularly high noise-to-signal ratio for that reason. This becomes more pronounced as the substrate concentration increases, making it difficult to detect changes in the current at high substrate concentrations.

3.2. Overview of data obtained from modeling procedures

The use of computer-driven non-linear regression has been previously postulated [23,24] and subsequently used in a number of biochemical studies [25] including enzyme kinetics [26–30]. It has the distinct advantage of objectively weighting errors in the data over the whole dataset, rather than exaggerating errors at low substrate concentrations (as occurs when data is normalized to the Lineweaver–Burke and Eadie–Hofstee plots [24] providing more robust overall estimations [23]. The use of iterative seeking-algorithms, such as those found in Microsoft Office's "Solver" add-in for non-linear regression curve-fitting has been previously performed [31,32] and the various adjustable parameters explained [31].

Table 2 displays the extracted values comparing the K_m, i_{max}, and sensitivity determined from chronoamperometric data obtained for all the laccase-modified surfaces investigated, when calibrated using hydroquinone. The i_{max} determinations and linear-range sensitivities were related to the electrode surface area, as both I (used in the calculation of the linear range sensitivities) and the I_{max} (Eq. (1)) are inherently related to the concentration of enzyme immobilized onto the electrode surface [18] which is, in turn, related to the real (microscopic) surface area of the electrode. K_m, as a ratio of combined enzyme-substrate association/dissociation rates, has no dependence on either concentration of enzyme or rate of diffusive response.

Laccases isolated from *T. versicolor* have previously been shown to have optimum K_m values ranging from between 37 and 155 μM, when soluble. Other *Trametes* species have optimum K_m values ranging from the low (<4) to high (>200) μM range. This is dependent on the selection of phenolic substrate and pH [33], but is within the range of the K_m values provided by the models for all surfaces investigated (see Fig. 2). While an increase in the apparent K_m of an enzyme is noted upon immobilization [2,3], an increase in the linker length between the support and the enzyme decreases the apparent K_m of the immobilized enzyme approximately half of the original value (~200 μM for both SAM 1.1 and SAM 2.1, compared to ~100 μM for SAM 1.3 and SAM 2.3). Similar results have been noted in literature when applying linkers connecting immobilized enzymes to solid supports [2,4]. This alteration is attributed to the adoption of a more solvated (i.e. optimal) conformation of the protein when the attached biomolecule is lifted from the support structure, [4], or increased accessibility of substrates to the catalytic sites in the immobilized film structure [34].

The anticipated close proximity of the enzyme layer to the electrode surface (less than 30 nm) relative to the rapid diffusional coefficients of hydroquinone in aqueous solutions (8.5×10^{-6} cm^2 s^{-1}) [17] resulted in a rapid response time. This, coupled to the close proximity of the enzyme to the transducer, relative to the thickness of the diffusional layer, δ, ensured that the current was fairly representative of the formation of product within the enzyme layer [27]. Increases in the distance between the electrode and enzyme layer (as a function of increasing linker length) may have resulted in the diffusion of some *p*-benzoquinone into the bulk solution, but such calculations are outside the scope of this research paper, and are probably insignificant due to the fact that the anticipated increase of distance from the electrode surface is in the nanometer range, and i_{max} was determined to be comparable to V_{max} for the purposes of this paper [27].

The findings reported in Table 2 show that both i_{max} and biosensor sensitivity were highest for SAM 1 films, relative to any other surface. The addition of linkers in both SAMs 1 and SAMs 2 increased both values, relative to SAMs 1.1 and SAMs 2.1, respectively. The sole exception was i_{max} values of SAM 1.2. Interestingly, while there is a decrease in the i_{max} for SAM 1.2 (relative to SAM 1.1), sensitivity is, in fact, enhanced with an increase in linker length, from an average of 4.8–8.4 nA μM^{-1} cm^{-2} between these surfaces. A strongly linear behaviour ($R^2 > 0.99$) was noted when comparing detection sensitivity of a given surface with the ratio of i_{max}/K_m values, equivalent to catalytic rate constant, V_{max}/K_m (data not shown). Thus, an improvement in biosensor sensitivity can be attributed to the decrease in the apparent K_m values of the laccase-modified surfaces, as opposed to only an improvement in the apparent i_{max}.

3.3. Integration of QCM-D data analysis with electrochemical kinetic parameters

Of great interest to this research was examining whether the rheological data provided through the QCM-D data (Paper 1 of this series) could be reconciled with the kinetic parameters elucidated through electroanalysis of the fabricated biosensors (Section 3.3 of this paper). Due to the differences inherent in both the immobilization method (with SAM 1 and Au electrodes making use of physical adsorption as the attachment parameter) and the film properties, trends in this section were only tracked between 3 categories: (1) differences between physically adsorbed and covalently attached protein films (2) between SAM surface of with differing linker lengths i.e. SAMs 1.1–1.3 and SAMs 2.1–2.3, respectively and (3) differences occurring between SAM 1 surfaces and SAM 2 surfaces.

Of the two rheological parameters (film shear and film viscosity) extracted from QCM-D measurement, viscosity was selected for the comparison between physical film parameters and immobilized enzyme kinetics. Increases in solution viscosity have been linked to the denaturation of dissolved proteins in previous research, for cited reasons of protein aggregation and conformational changes between the native and denatured state [35,36]. Secondly, literature has cited concerns regarding the accurate determination of film shear modulus through the Voigt-model [37] using QCM-D technology. Shear modulus values are therefore used as general

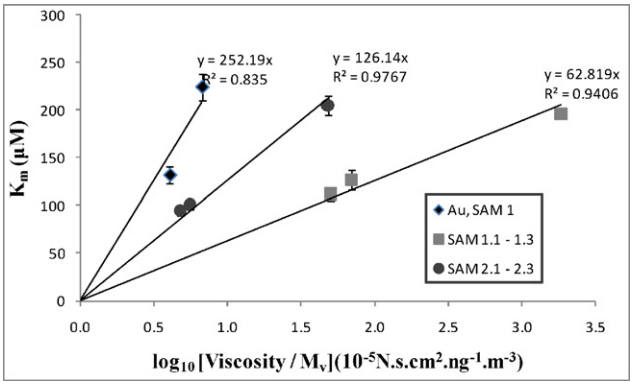

Fig. 3. Comparison between the K_m values (extracted from immobilized enzyme kinetics) determination to the logarithm of the average viscosity per unit mass of surfaces (extracted from QCM-D studies). *Y*-intercepts forced through the origin for linear regression of the data. Error bars represent standard deviation from the mean, $n \geq 3$.

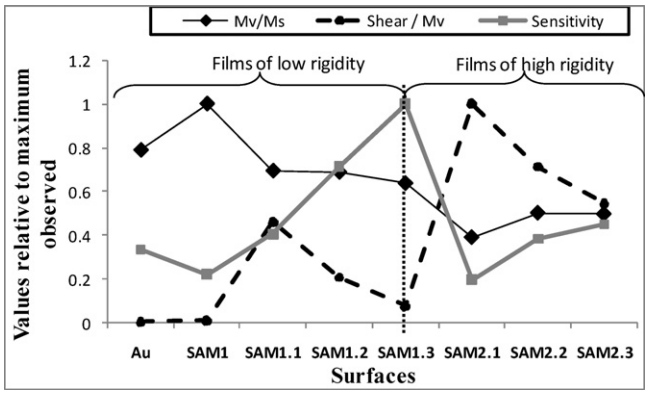

Fig. 4. Relative values of the immobilized film parameters shear modulus as a function of bound mass (Shear/M_V), ratio of Voigt mass to Sauebrey Mass (M_V/M_S) and average detection sensitivities (i/K) of the films with regard to HQ detection (Sensitivity). Data plotted in black indicates values drawn from QCM-D analysis of immobilized enzyme films (Paper 1). Data plotted in grey indicates values drawn from kinetic estimation of immobilized films' catalytic oxidation of HQ, as reported in this Paper. Cut-off values distinguishing high shear from low shear films was set $>2.5 \times 10^3$ N cm^2 ng^{-1} m^{-3}.

indicators of film rigidity, rather than absolute numerical values henceforth.

Theoretically, if one interprets viscosity as consisting of contributions arising from both the method of attachment and the extent of protein unfolding following immobilization, then the relationship between the viscosity (normalized relative to the bound mass) will provide an indication of the degree of denaturation undergone by attaching proteins, when categorised by the different surface types (i.e. adsorbed vs. covalent attachment, SAM type 1 vs. SAM type 2). The degree of denaturation undergone would also be represented as differences between K_m. Fig. 3 displays a comparison of the K_m values to the [mass-normalized] viscosity values obtained during QCM-D analysis for these three categories (Part 1).

Fig. 3 displays that strongly linear behaviour is noted between the surface types when comparing the K_m to the mass-normalized film viscosities. Linear correlations for 4-point trends for enzyme films immobilized onto SAM types 1.1–1.3 and 2.1–3.3 have R^2 values >0.94, and the 3-point correlation for the physically adsorbed enzyme films have $R^2 > 0.8$. The findings of Fig. 3 indicate that the decreases in attached laccase film viscosities through the use of linkers are linked to the decreases of K_m values observed at the same SAM amendments (Table 2), although the trends observed are restricted between the basal surfaces as outlined above. This strongly indicates that the anticipated decrease in enzyme denaturation due to linker inclusion is represented, in part, by the decreases in film rigidity/viscosity noted for during rheological comparison of the films immobilized onto the different surfaces.

While the Sauerbrey Mass (M_S) (Paper 1 of this series) contains a contribution from trapped/coupled water within the protein film, the Voigt Mass (M_V) is considered to be a more accurate estimation as it corrects for the viscoelasticity of the film. Increasing film softness results in an underestimation of M_S; in addition to which is acknowledged that the M_S imperfectly accounts for film swelling in the solvent [37]. Thus, to a very limited extent, the ratio of M_V compared to M_S provides some index of the relative softness and degree of film swelling exhibited by the immobilized enzyme films. Since both of these factors have contributions arising from protein–solvent interaction, M_V/M_S could therefore be taken as a crude estimation of the relative degree of solvation of the immobilized proteins, at least, when considering surfaces differing by the number of linkers connecting proteins to the gold electrode. Similar data treatments for estimating the level of film hydration via the differences occuring between M_V and M_S have been advanced in the literature [38].

When comparing the ratio of (M_V/M_S) to the i/K (sensitivity being considered analogous to i/K) values for immobilized laccase films, two opposing trends are evident – an inverse trend between (M_V/M_S) and HQ detection sensitivity for immobilized films exhibiting low shear modulus (i.e. low rigidity) properties and a positive trend for those possessing higher shear values, as determined by modeling of QCM-D results. Fig. 4 depicts the relational trends occurring between film shear (normalized to mass gain, as

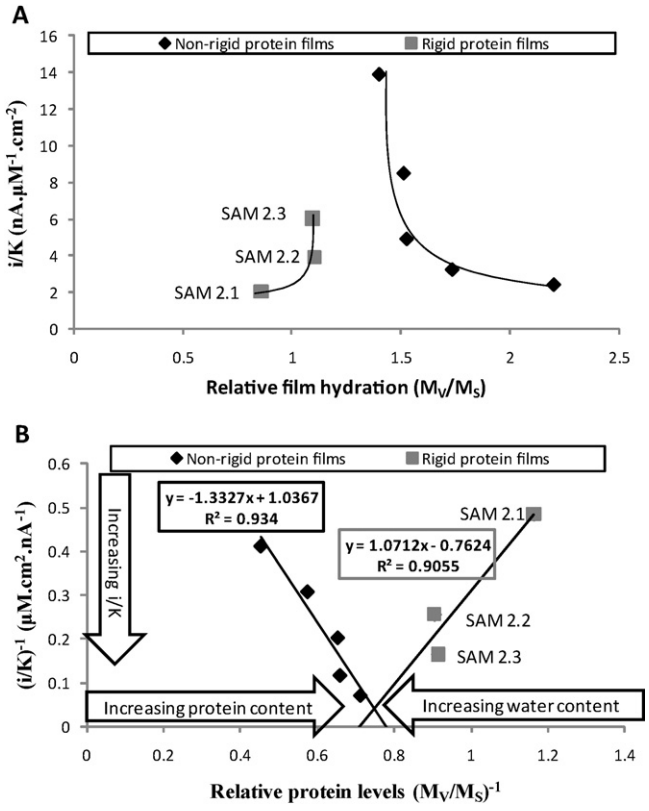

Fig. 5. Comparisons between i/K and relative film hydration values (M_V/M_S) obtained from combined kinetic and rheological analysis of the investigated surfaces. (A) i/K vs. (M_V/M_S) Lines drawn here are intended to show the asymptotic behaviour of the two separate film structures (rigid and non-rigid protein layers) to guide the user. (B) Reciprocal of (i/K) plotted against the reciprocal of (M_V/M_S). Arrows depict trends in values which are discussed further in-text.

was performed for viscosity, Fig. 3), the (M_V/M_S) ratio and the detection sensitivities for the surfaces examined.

Fig. 5A displays compasrisons between i/K values and the ratio of M_V/M_S (here putatively termed "relative film hydration") obtained for the surfaces studies, while Fig. 5B displays the reciprocal of i/K $(i/K)^{-1}$ against the reciprocal of M_V/M_S i.e. the relative protein levels present in films.

Due to the exponential dependence of i/K against the relative hydration levels (Fig. 5A), the reciprocal of both values were plotted against each other in order to linearise the noted dependences (Fig. 5B). Strongly linear, but opposing trends were noted when comparing the reciprocal of the i/K value to the relative protein content of the film (Fig. 5B). These two separate trends result from the two separate behaviours categorised in Figs. 5B and 4. Firstly, a decrease in relative hydration levels within non-rigidly attached films (i.e. an increase in relative protein mass of highly solvated films) increases the detection sensitivity, most likely through the inclusion of more catalytic protein within the film. This correlation occurs for both laccases attached to the electrode surfaces via physical adsorption, and for SAMs 1.1–1.3. However, in the case of rigidly attached (i.e. distorted/partially denatured) protein films, an increase in relative hydration levels also increases the i/K values, through a decrease in the degree of denaturation undergone by catalytic proteins during the attachment process. In addition to conformational alterations, increased hydration levels may also indicate the increased degree of accessibility of the substrate to the immobilized enzyme film [34].

4. Conclusions

It must be noted at this juncture that the scope of this research was not to design a satisfactory biosensor for its functionality – this form of biosensor is primarily fabricated in order to contrast the operating parameters of the functional biosensor with the salient rheological parameters and the other film properties determined from the QCM-D (as displayed in Part I of this two paper series). Hence, the use of this laccase fulfills the function of a "model" protein–film system.

Analysis of the biochemical kinetics of laccase attached to the various surfaces investigated indicated that, for both SAM 1-type and SAM 2-type surfaces, an increase in linker length lead to a significant decrease in the apparent K_m values of the enzyme film, accompanied by a significant increase of the detection sensitivity for the detection of HQ substrate. Additionally, a general increase in i_{max} was noted with an increase in linker length (SAMs 2.1–2.3, SAM 1.3 compared to SAM 1.1). Values for i_{max} and detection sensitivities were found to increase with a decrease in the lateral density of linkers (SAMs 1 compared to SAMs 2). Biosensor sensitivities increase significantly with the addition of linkers for all surfaces investigated, most likely due to the significant decreases in K_m values noted with increasing spacer-arm length. Linker-modified variants of SAM 2 surfaces (i.e. SAMs 2.2, 2.3) shows overall decreased sensitivities compared to SAM 1 surfaces, probably due to the aforementioned multiple attachments occurring between surface and enzymes [39]. Indeed, HQ detection sensitivity for laccase immobilized onto SAM 1.3 surfaces is nearly 6 times that of SAM 2.1 and more than three times that of the physically adsorbed surfaces (Au and SAM 1).

Analyses of the combined data extracted from QCM-D and the immobilized enzyme kinetics indicate considerations of bound protein mass alone are insufficient to predict the final parameters of the bound macromolecules and that inclusion of the rheological parameters obtained from QCM-D are necessary in order to correlate the enzyme kinetics of laccase films with the physical film parameters. Trends observed between QCM-D and immobilized enzyme kinetic studies indicate that biosensor performance (i_{max} and biosensor sensitivity) is enhanced with those surfaces that exhibit decreased shear/viscosity (e.g. SAMs 1.1–1.3), and that increasing rigidity tends to decrease biosensor performance, independently of bound Voigt mass.

Protein film viscosity was found to negatively influence the K_m of the resultant laccase-bound surfaces. When viscosity (in the form of the average viscosity per unit bound mass) was related to the K_m, a positive correlation was observed between the K_m and mass-normalized viscosity was found to occur, although this trend was restricted between surface types and the method of protein attachment used. Nevertheless, this is an indication that film viscosity, when assessed carefully, can predict the level of denaturation undergone by the proteins during the attachment phase. The degree of protein hydration (indicated by the ratio of Voigt-modeled mass to Sauerbrey mass) was found to correlate to the detection sensitivity. For non-rigid protein films, a decrease in this value (i.e. an increase in film protein content) trended with an increase in detection sensitivity, while an increase in the hydration level at very rigid protein films (SAMs 2.1–2.3) resulted in an increase in detection sensitivity. The addition of rheological parameters appears to better nuance the differences arising in bound enzyme kinetics due to the differences between immobilization strategies and allow for more in-depth comparisons that determinations of the bound mass alone cannot show.

While other studies have also linked the film structure of a monolayer of immobilized protein to its function, QCM-D offers the opportunity to assess the physical characteristics of that film in a more direct fashion than some of the other methods (AFM, STM, Raman–UV–vis-spec, etc.). Integrating both the inferred rheological properties of the film derived from QCM-D and comparing them with those determined by electrochemical monitoring of the immobilized laccase monolayer is a potentially viable tool in biosensor design.

Acknowledgements

The authors acknowledge the support of Department of Science & Technology/Mintek Nanotechnology Innovation Centre of South Africa and National Research Foundation (SA) for funding.

References

[1] Royer GP. Immobilised enzymes. In: Royer GP, editor. Fundamentals of enzymology: rate enhancement, specificity, control and applications. USA: John Wiley and Sons Ltd.; 1982. p. 181–94.
[2] Bayramoğlu G, Altınok H, Bulut A, Denizli A, Arıca MY. Preparation and application of spacer-arm-attached poly(hydroxyethyl methacrylate-co-glycidyl methacrylate) films for urease immobilization. React Funct Polym 2003;56:111–21.
[3] Bayramoğlu G, Arica MY. Enzymatic removal of phenol and p-chlorophenol in enzyme reactor: Horseradish peroxidase immobilized on magnetic beads. J Hazard Mater 2008;156:148–55.
[4] Lowe CR. Immobilized lipoamide dehydrogenase 2. Properties of the enzyme immobilized to agarose through spacer molecules of various lengths. Eur J Biochem 1977;76:401–9.
[5] Kim G-Y, Cuong NM, Cho S-H, Shim J, Woo J-J, Moon S-H. Improvement of an enzyme electrode by poly(vinyl alcohol) coating for amperometric measurement of phenol. Talanta 2007;71:129–35.
[6] Klis M, Maicka E, Michota A, Bukowska J, Sek S, Rogalski J, et al. Electroreduction of laccase covalently bound to organothiol monolayers on gold electrodes. Electrochim Acta 2007;52:5591–8.
[7] Freire RS, Durán N, Kubota LT. Effects of fungal laccase immobilization procedures for the development of a biosensor for phenol compounds. Talanta 2001;54:681–6.
[8] Mateo C, Grazú V, Pessela BCC, Montes T, Palomo JM, Torres R, et al. Advances in the design of new epoxy supports for enzyme immobilization–stabilization. Biochem Soc Trans 2007;35:1593–601.
[9] Cabaj J, Sołoducho A, Chyla J, Bryjak K, Zynek. The characterization of ordered thin films built of immobilized phenoloxidases. Sens Actuators B: Chem 2009;136:425–31.
[10] Mazur M, Krysiński P, Michota-Kamińska A, Bukowska J, Rogalski J, Blanchard GJ. Immobilization of laccase on gold, silver and indium tin oxide by

zirconium–phosphonate–carboxylate (ZPC) coordination chemistry. Bioelectrochemistry 2007;71:15–22.
[11] Voinova MV, Rodahl M, Jonson M, Kasemo B. Viscoelastic acoustic response of layered polymer films at fluid-solid interfaces: continuum mechanics approach. Physica Scripta 1999;59:391–6.
[12] Höök M, Rodahl B, Kasemo P, Brzezinski. Structural changes in hemoglobin during adsorption to solid surfaces: effects of pH, ionic strength, and ligand binding. Proc Natl Acad Sci USA 1998;95:12271–6.
[13] Fogel R, Mashazi P, Nyokong T, Limson J. Critical assessment of the quartz crystal microbalance with dissipation as an analytical tool for biosensor development and fundamental studies: metallophthalocyanine–glucose oxidase biocomposite sensors. Biosens Bioelectron 2007;23:95–101.
[14] Carvalhal RF, Freire RS, Kubota LT. Polycrystalline gold electrodes: a comparative study of pretreatment procedures used for cleaning and thiol self-assembly monolayer formation. Electroanalysis 2005;17:1251–9.
[15] Royer GP. Rate equations for enzyme-catalyzed reactions. In: Royer GP, editor. Fundamentals of enzymology: rate enhancement, specificity, control and applications. USA: John Wiley and Sons Ltd.; 1982. p. 45–9.
[16] Quan D, Kim Y, Shin W. Characterization of an amperometric laccase electrode covalently immobilized on platinum surface. J Electroanal Chem 2004;561:181–9.
[17] French RW, Marken F. Growth and characterisation of diffusion junctions between paired gold electrodes: diffusion effects in generator–collector model. J Solid State Electrochem 2009;13:609–17.
[18] Miller A, Tanner J. Kinetics catalysis. In: Miller A, Tanner J, editors. Essentials of chemical biology. Barcelona: John Wiley & Sons, Ltd.; 2008. p. 408–13.
[19] Barton SC, Pickard M, Vazquez-Duhalt R, Heller A. Electroreduction of O_2 to water at 0.6 V (SHE) at pH 7 on the 'wired' *Pleurotus ostreatus* laccase cathode. Biosens Bioelectron 2002;17:1071–4.
[20] Ding S-N, Holzinger M, Mousty C, Cosniera S. Laccase electrodes based on the combination of single-walled carbon nanotubes and redox layered double hydroxides: towards the development of biocathode for biofuel cells. J Power Sources 2010;195:4714–7.
[21] Vianello F, Cambria A, Ragusa S, Cambria MT, Zennaro L, Rigo A. A high sensitivity amperometric biosensor using a monomolecular layer of laccase as biorecognition element. Biosens Bioelectron 2004;20:315–21.
[22] Rahman MA, Noh H-B, Shim Y-B. Direct electrochemistry of laccase immobilized on Au nanoparticles encapsulated-dendrimer bonded conducting polymer: application for a catechin sensor. Anal Chem 2008;80:8020–7.
[23] Sagnella GA. Fitting linear models to structure-activity data. Trends Biochem Sci 1985;10:100–3.
[24] Leatherbarrow JR. Using linear and non-linear regression to fit biochemical data. Trends Biochem Sci 1990;15:455–8.
[25] Coons DM, Boulton RB, Bisson LF. Computer-assisted nonlinear regression analysis of the multicomponent glucose uptake kinetics of *Saccharomyces cerevisiae*. J Bacteriol 1995;177:3251–8.
[26] Stojan J. Analysis of progress curves in an acetylcholinesterase reaction: a numerical integration treatment. J Chem Inf Comput Sci 1997;37:1025–7.
[27] Gooding JJ, Erokhin P, Hibbert DB. Parameters important in tuning the response of monolayer enzyme electrodes fabricated using self-assembled monolayers of alkanethiols. Biosens Bioelectron 2000;15:229–39.
[28] Johnson KA. Introduction to kinetic analysis of enzyme systems. In: Johnson KA, editor. Kinetic analysis of macromolecules. United Kingdom: Oxford University Press; 2003. p. 1–18.
[29] Goudar CT, Harris SK, McInerney MJ, Suflita JM. Progress curve analysis for enzyme and microbial kinetic reactions using explicit solutions based on the Lambert W function. J Microbiol Methods 2004;59:317–26.
[30] Walsh R, Martin E, Darvesh S. A versatile equation to describe reversible enzyme inhibition and activation kinetics: modeling β-galactosidase and butyrylcholinesterase. Biochim Biophys Acta 2007;1770:733–46.
[31] Walsh S, Diamond D. Non-linear curve fitting using microsoft excel solver. Talanta 1994;42:561–72.
[32] Lin C-W, Chen S-Y, Cheng Y-W. Effect of metals on biodegradation kinetics for methyl tert-butyl ether. Biochem Eng J 2006;32:25–32.
[33] Baldrian P. Fungal laccases—occurrence and properties. FEMS Microbiol Rev 2006;30:215–42.
[34] Arshady R, Review:. Beaded polymer supports and gels II. Physico-chemical criteria and functionalisation. J Chromatogr 1991;586:199–219.
[35] McKenzie HA, Smith MB, Wake RG. The denaturation of proteins: I. Sedimentation, diffusion, optical rotation viscosity and gelation in urea solutions of ovalbumin and bovine serum albumin. Biochim Biophys Acta 1963;69(1963):222–39.
[36] Tamiya T, Okahashi N, Sakuma R, Aoyama T, Akahane T, Matsumot JJ. Freeze denaturation of enzymes and its prevention with additives. Cryobiology 1983;22(1985):446–56.
[37] Johannsmann D. Viscoelastic, mechanical, and dielectric measurements on complex samples with the quartz crystal microbalance. Phys Chem Chem Phys 2008;10:4516–34.
[38] Paul S, Paul D, Basova T, Ray AK. Studies of adsorption and viscoelastic properties of proteins onto liquid crystal phthalocyanine surface using quartz crystal microbalance with dissipation technique. J Phys Chem C 2008;112:11822–30.
[39] Butterfieled A, Bhattacharyyab D, Daunerta S, Bachasa L. Catalytic biofunctional membranes containing site-specifically immobilized enzyme arrays: a review. J Memb Sci 2001;181:29–37.